In−silico modelling and identification of a possible inhibitor of H1N1 virus

Chandrabhan Seniya[1*], Ghulam Jilani Khan[2], Richa Misra[1], Vaibhav Vyas[1], Shruti Kaushik[1]

[1]*Department of Biotechnology, Madhav Institute of Technology and Science, Race Course Road, Gola Ka Mandir, Gwalior (M.P.) India*

[2]*Department of Biotechnology, L.N. Mithila University, Darbhanga, Bihar−846004, India*

PEER REVIEW

ABSTRACT

Objective: To find the neuraminidase H1N1 inhibition potential of 4−hydroxypanduratin A and its derivatives along with associated binding mechanism through virtual screening and molecular docking.

Methods: Initially, the structural templates for neuraminidase proteins were identified from structural database using homology search and performed homology and *ab initio* modeling to predict native 3D structure using Modeller 9.10 and I−TASSER server, respectively. The reliability of the three−dimensional models was validated using Ramachandran plot. The molecular docking was performed using Autodcok 4.2 and molecular interactions were analyzed through PyMol, Chimera and LigPlot.

Results: The neuraminidase protein sequences of ADH29478, ADD85918, AEM62864 (2009) and AFO38701 (2011) from India were modeled and validated. 4−hydroxypanduratin A and its 88 derivatives were docked in to active binding pockets of neuraminidase. The guanidine group of residues Arg152 and Trp179 of ADH29478 (Chennai) and AFO38701 (Gwalior) neuraminidase models present in the hydrophilic domain (−OH and =O groups) was found to have molecular interactions with high binding affinities of −7.40 kcal/mol and −8.66 kcal/mol, respectively to 1−(2,4−dihydroxyphenyl)−3,3−diphenylpropan−1−one (CID: 19875815) than other FDA approved drugs such as oseltamivir, zana−mivir, and peramivir.

Conclusions: 1−(2,4−dihydroxyphenyl)−3,3−diphenylpropan−1−one will be a breakthrough for further drug development against swine flu.

1. Introduction

The derivatives of 4−hydroxypanduratin A are natural plant secondary metabolites of *Boesenbergia pandurata* (Roxb.) Schltr. (Syn. *Kaempferia pandurata* Roxb.) (Fingerroot) which are a member of the Zingiberaceae family (ginger). It is widely used as a medicinal plant and has been reported to possess pharmacological importance such as anti inflammatory[1], anti angiogenic[2], neuroprotective, chemoprotective[3], and antioxidant[4] activities. The 4−hydroxypanduratin A has shown promising inhibitory activity against dengue virus NS2B/NS3 protease[5,6] and Japanese encephalitis virus, a major cause of acute encephaltis in Asia[7]. Influenza viruses which caused the pandemics in 1918 and in 2009, due to the severity of the change in the hemagglutinin and neuraminidase of the

influenza H1N1 sequence, was commonly named swine flu as it emerged from swines (pigs). Since 2009 new strain of the influenza A virus (H1N1) has rapidly spread to many countries from the initial outbreak in South America. Swine flu is a contagious disease caused by H1N1 virus which leads to severe respiratory tract infection and other complications such as pneumonia, bronchitis in humans. The World Health Organization reported 12787 confirmed cases and 413 death cases, all caused by H1N1, on 18 Oct 2009[8]. Influenza virus H1N1 consists of two glycoproteins, hemagglutinin and neuraminidase. Hemagglutinin facilitates the influenza virus to attach to a host cell during the initial infection and viral RNA enters the cell by endocytosis. Neuraminidase cleaves α–ketosidic linkage between the sialic acid (N–acetylneuraminic) and an adjacent sugar residue and release of the progeny virions from the infected host cells. In addition, it has a function as importer facilitating the early process of the infection of lung epithelial cells by the influenza virus[9]. Neuraminidase has been an attractive target for the development of novel anti–influenza drugs because of its essential role in influenza virus replication and its highly conserved active sites[10–16]. The inhibition of neuraminidase is useful in prevention of H1N1 and could serve as potential drug target. Due to development of resistance in many strains of H1N1, the Food and Drug Administration (FDA) approved neuraminidase inhibitor drugs such as oseltamivir[17–19] and zanamivir[20] and due to several sides effects like nausea, vomiting, abdominal pain and headache, rash and sometimes allergic reactions including anaphylaxis *etc.*, there is a call for new inhibitors against H1N1 influenza A virus with less or no side effects.

Neuraminidase inhibitors are a class of antiviral drugs targeted at the influenza virus, which work by blocking the function of the viral neuraminidase protein, thus preventing the virus from reproducing by budding from the host cell. Inhibition of neuraminidase function appears critical in limiting the progression of influenza virus infection in the host. Crystallographic analyses of neuraminidases have provided a platform for structure–based drug design. The amino acid sequence of the neuraminidase of ADH29478.1, ADD85918.1, AEM62864.1, and AFO38701.1 is known but the 3D structure is not available. Therefore, the 3D native structures were predicted by homology modelling and *ab initio* modelling through Modeller 9.10 and I–TASSER, respectively. The molecular docking simulations were performed on 4–hydroxy panduratin A and neuraminidase. 4–Hydroxypanduratin A and its 88 derivatives were docked on active site binding pocket residue Arg152 which is said to be conserved among all the neuraminidase H1N1. Docking has been used to predict the interactions between ligand and receptor. Since the ligand can bind with the binding site on the receptor molecule in several possible orientations, the goal of docking is to screen in favourable interactions against prohibitive ones[21].

2. Materials and methods

2.1. Materials

The neuraminidase protein sequences of ADH29478.1, ADD85918.1, AEM62864.1, and AFO38701.1 H1N1 strain were retrieved from NCBI Influenza Virus Resource database[22]. The neuraminidase protein sequences were retrieved by putting keywords by using keywords *viz.*, Type: A, Host: Human, Country/Region: India, Protein: neuraminidase, Subtype: H1 and N1, Sequence type: Protein. Lists of 80 protein sequence of neuraminidase of different regions of India have been retrieved.

2.2. Methods

2.2.1. Molecular modelling of neuraminidase
Molecular modeling of novel neuraminidase receptor proteins was performed using modeling server I–TASSER and Modeller 9.10[23]. Pair wise sequence alignment of template and target sequences were performed using BLASTp against Protein Data Bank (PDB) database. Structure refinement and energy minimization were performed with energy minimized. 3D structure files were prepared using Swiss PDB Viewer and Modeller 9.10 itself using the regularization macro. 3D structures were also predicted by I–TASSER and further verification of modelled structures was done using PROCHECK v3.4.4[24] for the overall and residue–by–residue geometry through Ramchandran plot.

2.2.2. Active binding site prediction
In–silico binding site characterization of ADH29478.1, ADD85918.1, AEM62864.1, and AFO38701.1 neuraminidase H1N1 were done using CASTp[25,26], Q–Site Finder[27] and compared by extensive literature search. Best active sites were selected by comparing prediction of CASTp algorithm and Q–Site Finder.

2.2.3. Ligand selection and preparation
About 88 analogues of 4–hydroxypanduratin A were collected from NCBI PubChem compound database on the basis of structure similarity and functionality as a pharmacophore and virtually screened on the basis of Lipinski's rule of 5[28]. The ligands were converted into PDB coordinate files using OpenBabel software. Ligand preparation involves the addition of hydrogen bonds, neutralization of the charge groups and removal of any miscellaneous structures from the ligand. The optimized lignads were subsequently used for docking.

2.2.4. Molecular docking
The 3D structures of modeled neuraminidase proteins were used to molecular docking with 3D structure of 4–hydroxy panduratin A and its derivatives using AutoDock 4.2 program. The receptors were prepared by assigning bond orders,

adding hydrogens, setting proper ionization states of residues, capping the termini, and so forth. The receptors were then refined with H–bond assignment (water orientations, at neutral pH), and energy was minimized with Gromos 43b1 force field. A grid for the protein was generated by using site around the centroids of selected residues. The ligands were prepared in ligprep with the following parameters force field: Gromos 43b1, ionization at target pH: 7.0±2.0, generate tautomers and stereo isomers with at most 32 ligands to be generated. Docking study was carried out using the empirical free energy function and the Lamarckian genetic algorithm. Autodock generates different conformers for each docking simulation. The result of docking simulation provided the orientation and specific position of best binding of the ligand in the active site, which were used to determine nearest neighbors, hydrogen bonding and Van der Waals interactions. After ensuring that protein and ligands are in correct form for docking, the receptor–grid files were generated using grid receptor generation program using Van der Waals scaling of the receptor at $0.6 \text{\AA}$ using Autogrid program in Autodock 4.2 and grid maps for the ligands were also generated to the target residue Arg152 and the 150 loop region enclosed in the grid box ($60 \text{\AA} \times 60 \text{\AA} \times 60 \text{\AA}$) with the grid point separation of $0.375 \text{\AA}$ [29]. Rigid state of docking was performed, initially using the "standard precision" method and further using the "xtra precision Lamarckian genetic algorithm" with standard docking protocol was used to find the most preferred pose where the ligand can bind to the receptor with lowest binding energy. The Python scripts in MGL tools package were used to analyze the docking results. The molecular structures of a protein or substrate could be visualized and analyzed by MGL tools. Python Molecular Viewer was used to observe the 3D structure and molecular interactions. The docking results were also analyzed using LIGPLOT and as per our previous study[30]. A single best conformation for each ligand was considered for further analysis.

3. Results

3.1. Protein modelling and validation

The neuraminidase protein sequences reported in NCBI for ADH29478.1, ADD85918.1, AEM62864.1 (2009) and AFO38701.1 (2011) from Chennai, Kolkata, Pune and Gwalior, respectively, were retrieved. Homology sequences search was done against quarry sequences using Basic Local Alignment Search Tool (BLASTp) against PDB database which was performed to identify the template sequence and the 3D structures for the target sequence but no significant hit with complete query coverage for template to build 3D model were found. The best template structure was identified PDB ID: 4B7R. Homology modelling was used to generate a reliable 3D model of neuraminidase (H1N1) protein using

Modeller 9.10 but none of the good quality models with appropriate folded conformations were predicted using PDB ID: 4B7R protein as a template. Therefore, the automated 3D structures of neuraminidase (H1N1) were again predicted based on the sequence–to–structure–to–function paradigm using I–TASSER (Figure 1). I–TASSER integrated web platform uses a composite approach for protein modelling combining *ab initio*, threading and comparative modelling[31]. In the first step, the query sequence was threaded through a non redundant sequence database to identify evolutionary relatives. A profile of homologous sequences was created to predict the secondary structure using PSIPRED[32]. The predicted secondary structure templates were ranked through LOMETS a meta threading server[33]. Templates were judged as per their Z score and top hits were considered for further evaluation. In the second step of structure prediction, the structure was built by assembling the fragments from different templates while the unaligned regions were predicted through *ab initio* modelling[34–36]. Monte Carlo Simulations were performed at different temperatures and low temperature to assemble the fragments and the structural trajectories were selected and clustered by SPICKER[37]. In the third step, the 3D model was refined by the closest PDB structure retrieved by TM align[38]. The accuracy of the predicted structure was analysed through the C–score[39] and TM–score[40].

3.2. Molecular docking simulation studies

The computational methods are simple and non–expensive which speed up the process of designing novel and potent therapeutic molecules with desired high biological potency. Docking is one of the commonly used computational methods for structure based drug designing[41]. Docking predicts the preferred orientation of a ligand with the binding site on a receptor. The strength of the interaction between ligand and receptor is measured in terms of experimentally defined inhibition constant Kd. Molecular docking is utilized for the prediction of protein ligand interaction and scoring function that predicts the binding affinity of the ligand to protein based on the complex geometry, here in our study the top 5 ligand (4–hydroxypanduratin A derivatives) having minimum energy were screened out as the possible inhibitors and were compared with them the FDA approved drug such as oseltamivir, zanamivir, and peramivir.

The neuraminidase story started in the early 1940s, almost a decade after the first human influenza virus was isolated. H1N1 cases reported in NCBI Influenza resource database from January 2000 to February 2013 were retrieved and a pie chart was prepared (Figures 2 and 3). The maximum cases have been reported in 2009 which were almost >60% of the collected cases followed by 2010 (9.2%). In this study, special focus was given to the H1N1 reported cases in India. About 80 cases have been retrieved which includes 14 cases from Chennai, 01 each from Delhi, Gwalior, Bareilly, Nasik, Jalna,
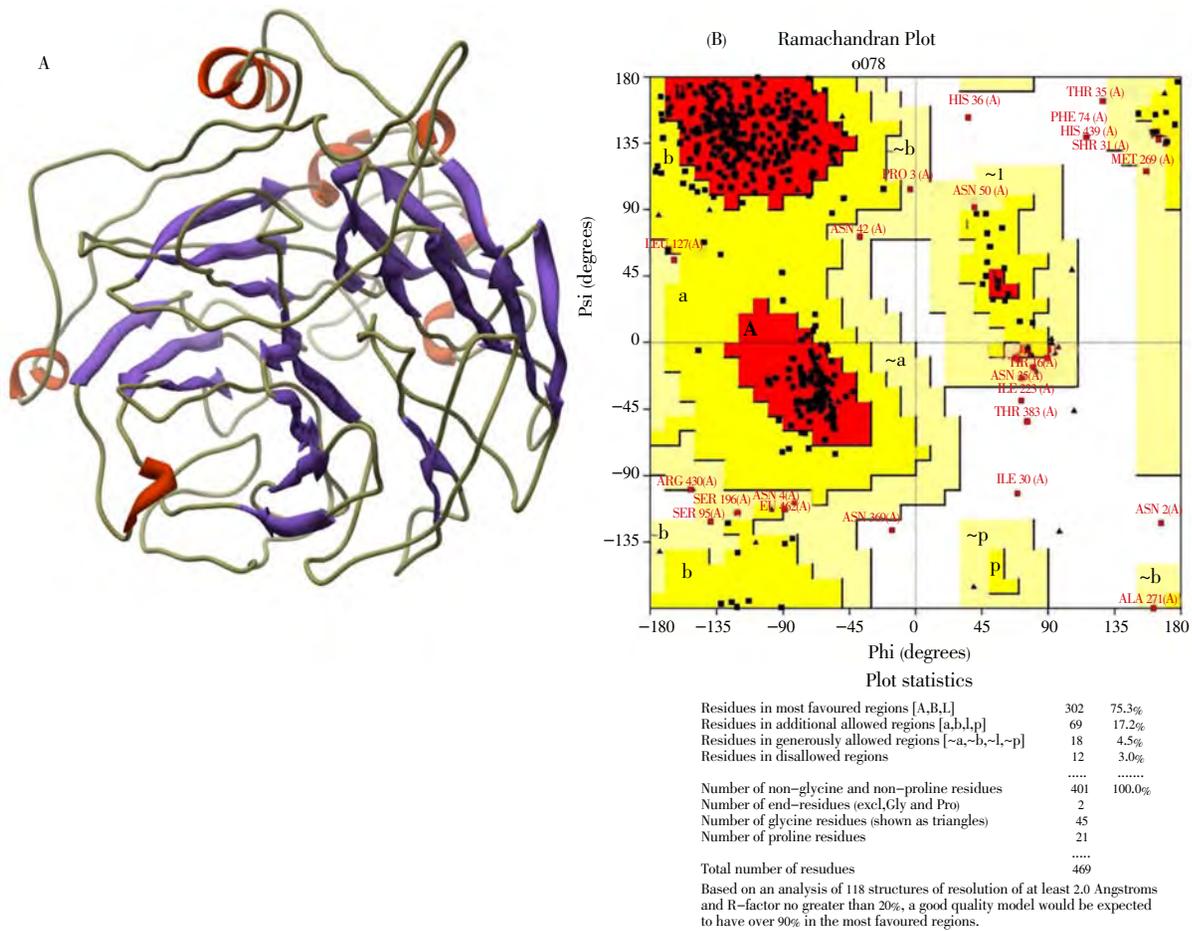
Figure 1. A–Predicted 3D structure, B–Ramchandran plot of neuraminidase H1N1 protein Chennai (ADH29478).
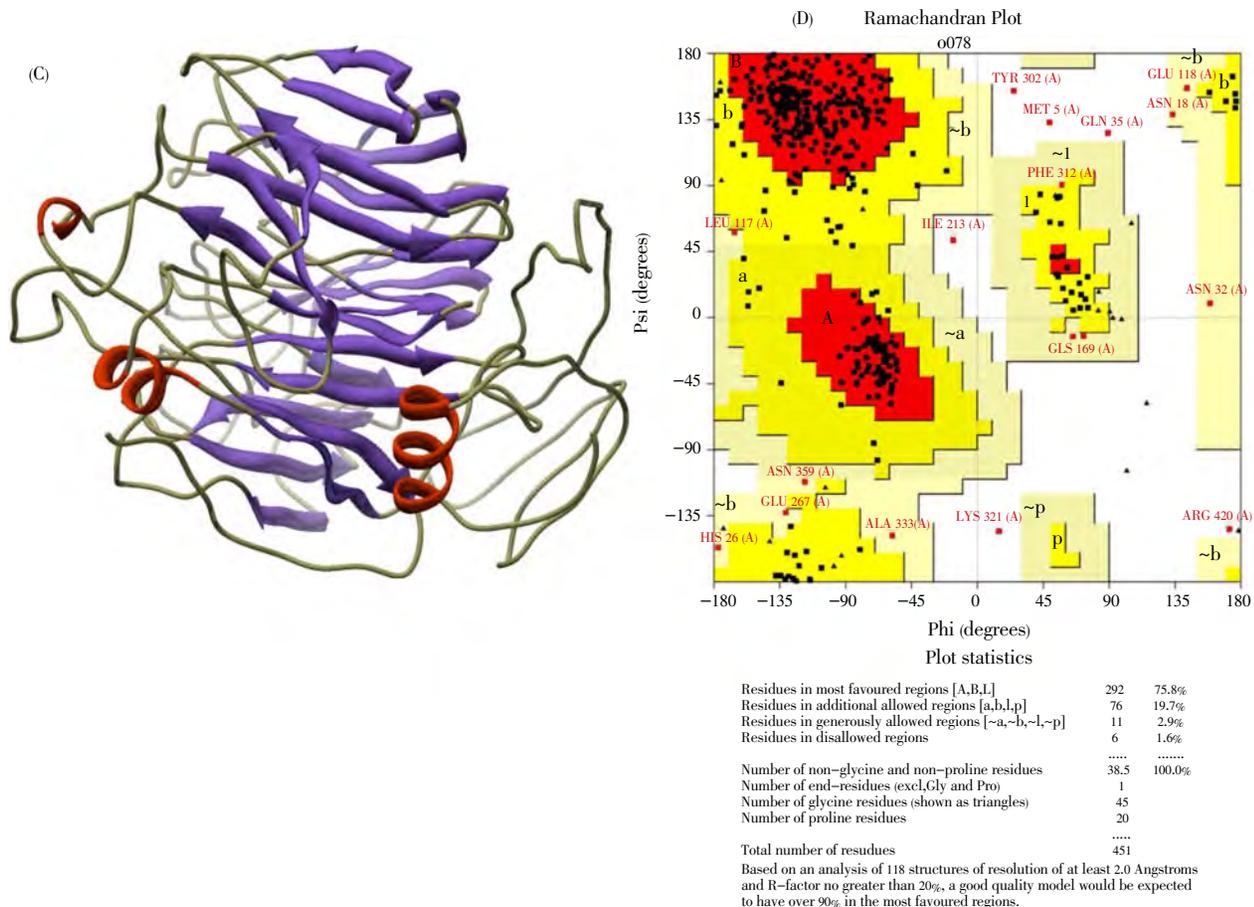

Figure 1. C–Predicted 3D structure, D–Ramchandran plot of neuraminidase H1N1 protein Kolkata (ADD85918).
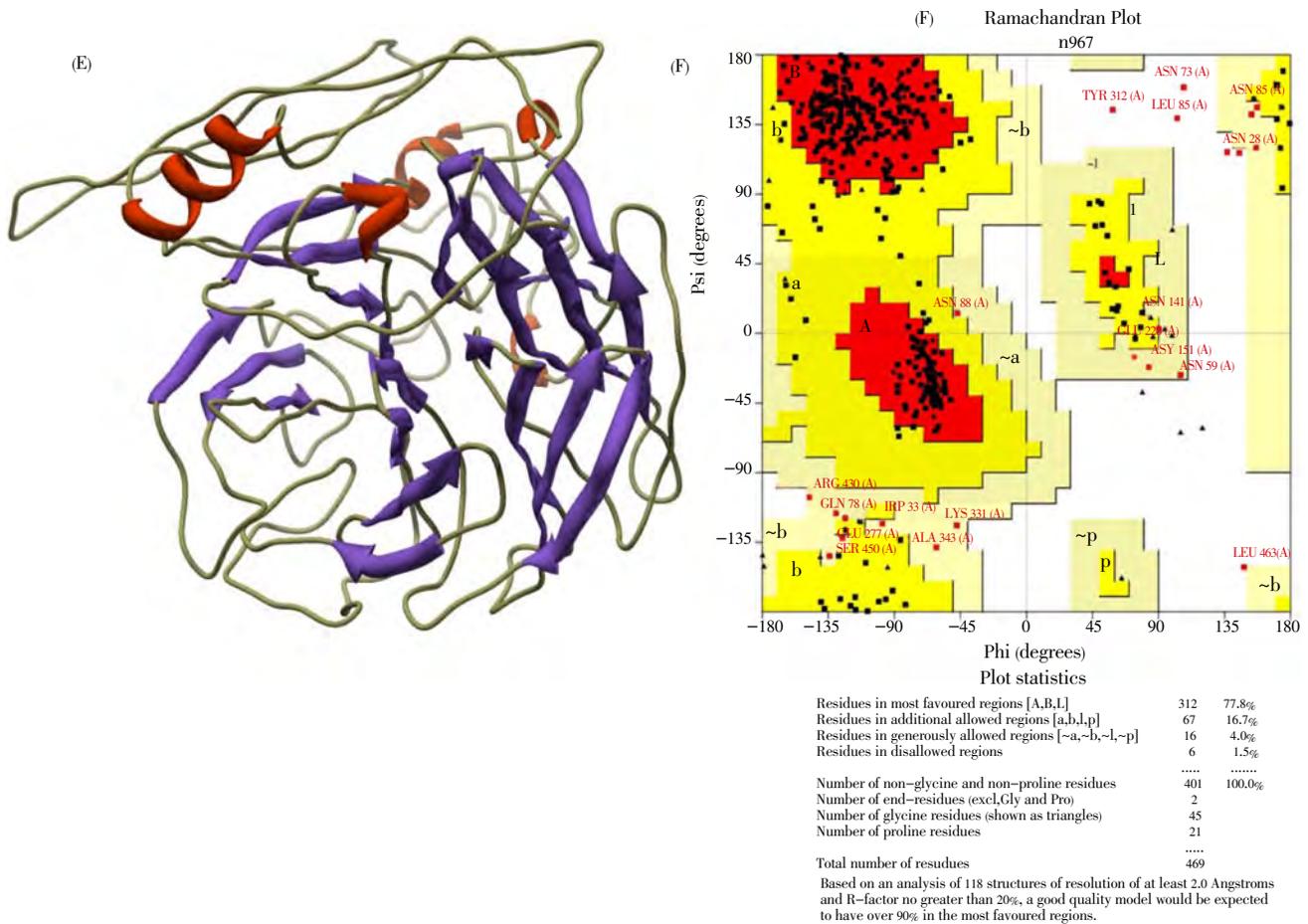
Figure 1. E–Predicted 3D structure, F–Ramchandran plot of neuraminidase H1N1 protein Pune (AEM62864).
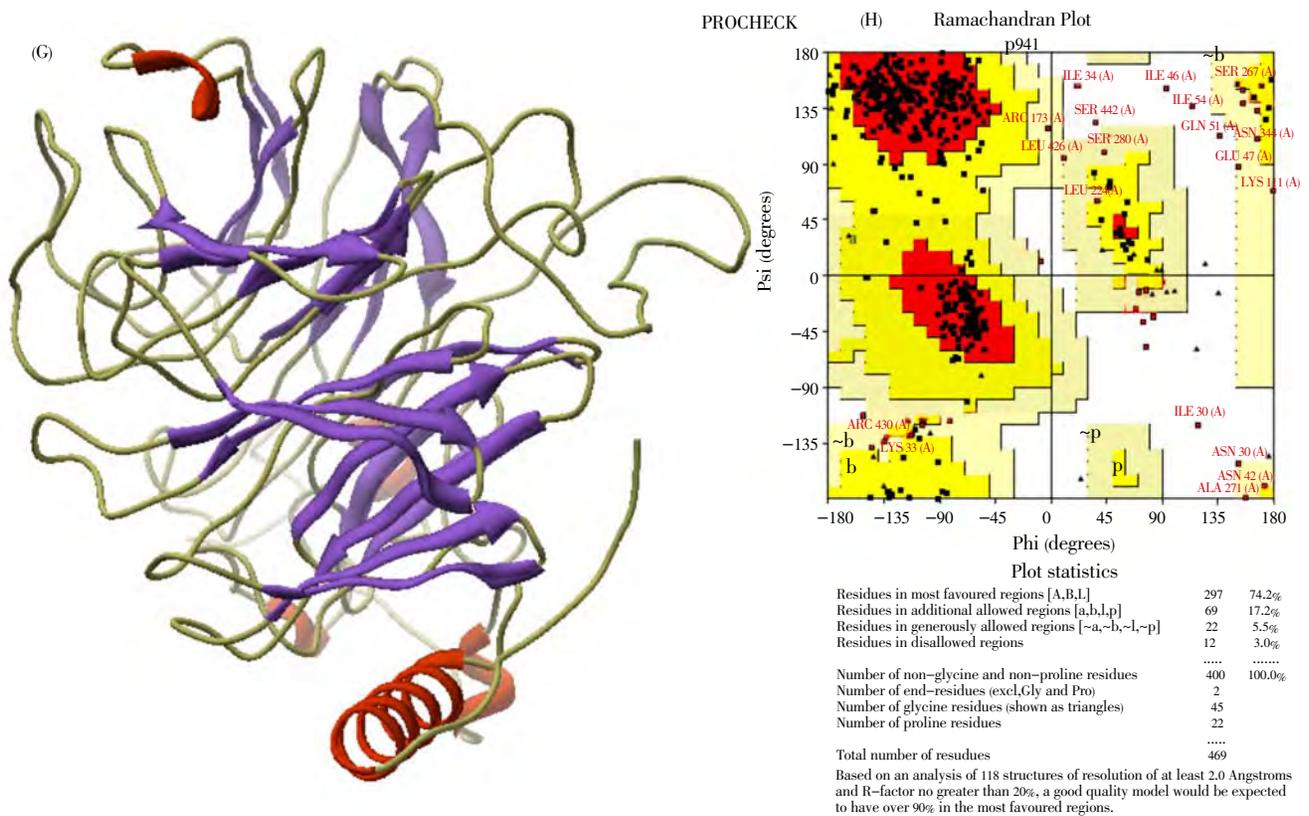

Figure 1. G–Predicted 3D structure, H–Ramchandran plot of neuraminidase H1N1 protein Gwalior (AFO38701).

Hyderabad, Vaddu, Ratnagir, 03 from Mumbai, 13 from Pune, and 35 from Kolkata (Figure 3) till today. More interestingly a maximum number of cases of 44% were reported in Kolkata, followed by 18% cases in Chennai, and 16% in Pune.
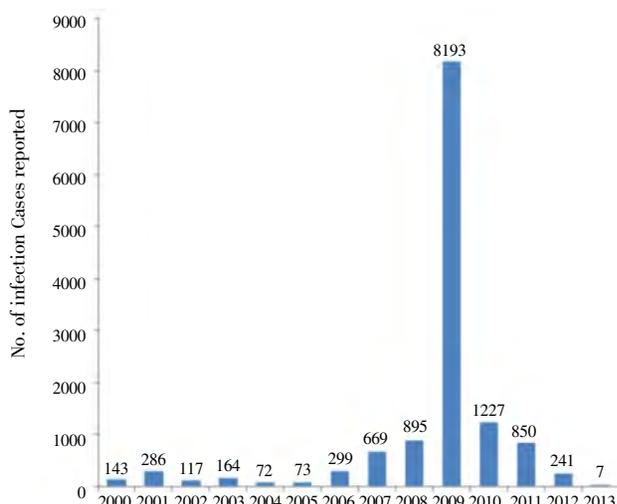

Figure 2. Worldwide H1N1 (neuraminidase) infection cases reported in NCBI Influenza resource database from January 2000–February 2013.
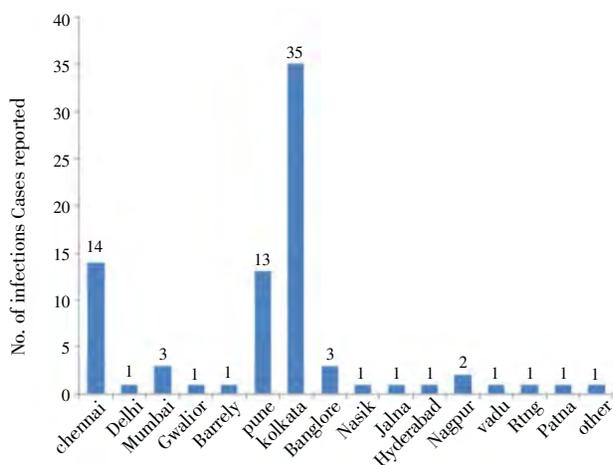

Figure 3. H1N1 (neuraminidase) infection cases reported from India in NCBI Influenza database from January 2000–February 2013.

The neuraminidase protein sequences of ADH29478.1, ADD85918.1, AEM62864.1 (2009) and AFO38701.1 (2011) from Chennai, Kolkata, Pune and Gwalior, respectively, were retrieved and homology modelling was used to generate a reliable 3D model of neuraminidase (H1N1) proteins using

Modeller 9.10 but none of the good quality models with appropriate folded conformations were predicted using PDB ID: 4B7R protein as a template. Therefore, the automated 3D structures of neuraminidase (H1N1) were again predicted based on the sequence–to–structure–to–function paradigm using I–TASSER (Figure 1). The stereochemical quality of the 3D structure predicted by I–TASSER was further verified using PROCHECK v3.4.4 for the overall and residue–by–residue geometry through Ramchandran plot. The peptide bond geometry (phi/psi torsion angles) of the protein backbone of predicted structure was determined.

The statistical analysis of Ramachandran plot shows 75.3%, 75.8%, 77.8%,74.2% residues in most favored regions, 17.2%, 19.7%, 16.7%, 17.2% in additionally allowed regions, 4.5%, 2.9%, 4.0%, 5.5% in generously allowed regions and only 3.0%, 1.6%, 1.5%, 3.0% residues in disallowed regions for all four models. Thus, altogether 92.5%, 95.5%, 94.5%, 96.9% of residues were placed in favored and allowed categories respectively in the four model predicted by I–TASSER is of good quality in terms of protein folding. These structures were further used as a model to study protein–ligand interactions (Figure 1).

3.2.1. Molecular interaction between 4–hydroxypanduratin A derivatives with neuraminidase of ADH29478 from Chennai

On the basis of molecular interactions shown by Ligplot and docking 1–(2,4–dihydroxyphenyl)–3,3–diphenylpropan–1–one (CID: 19875815) was identified as the best lead compound. The binding energy was found to be −7.40 kcal/mol, 03 hydrogen bond interaction with Arg152, Trp179, Ser196 and 04 hydrophobic interactions in the binding pocket cavity of ADH29478 (Table 1, Figure 4). Most interestingly the inhibition constant value of 3.75 μmol/L with the total intermolecular energy was −9.49 kcal/mol. This signifies that it would have high inhibition potential than other selected FDA approved bioactive drugs for swine flu such as oseltamivir (CID: 65028), zanamivir (CID: 60855), peramivir (CID: 154234) (Table 1). Additionally, CID: 19875815 was found interacting with 150 loop region, very near to binding cavity, such that it recognizes to enable more extensive interactions with the ligand, as well as with other active–site residues in the vicinity. These studies revealed structure conformational changes in 150 loop, secondary sialic acid binding site residues of neuraminidase.

Table 1

Characteristics of top 5 4–hydroxypanduratin A derivative inhibitors of neuraminidase H1N1 [ADH29478 (Chennai)] identified after molecular docking.

S. No.	CID	Molecular formulae	M. W. (g/mol)	Log P	Binding Energy score (kcal/mol)	Total inhibition constant Ki (μmol/L) at 298.15 K	Hydrogen bond interaction	Hydrophobic bond interaction	Total intermolecular energy (kcal/mol)
1	19875815	$C_{21}H_{18}O_3$	318.36	4.8	−7.40	3.75	3 (Arg152, Trp179, Ser196)	4	−9.49
2	42623682	$C_{16}H_{16}O_4$	272.29	3.9	−6.59	14.78	4 (Arg152, Trp179, Ser196, Asp199)	4	−8.38
3	20601635	$C_{15}H_{14}O_5$	274.26	2.9	−6.55	15.91	2 (Arg156, His144)	6	−8.63
4	10494301	$C_{18}H_{18}O_4$	298.33	4.4	−6.27	25.45	5 (Asp151, Arg156, Ser153, His144, Gln136)	2	−8.36
5	42607676	$C_{20}H_{22}O_4$	326.38	4.9	−6.04	37.62	1 (Arg152)	5	−8.72
Osel	65028	$C_{16}H_{28}N_2O_4$	312.40	1.1	−2.40	17470	2 (Arg152, Trp179)	4	−5.08
Per	154234	$C_{15}H_{28}N_4O_4$	328.40	0	−4.23	797.22	4 (Gly147, Ser153, Arg156, Gln136)	3	−6.91
Zan	60855	$C_{12}H_{20}N_4O_7$	332.30	−3.2	−5.15	166.57	6 (Asp151, Arg156, Gln136, Thr148, His 144)	4	−8.14

Osel=Oseltamivir, Per=Peramivir, Zan= Zanamivir.

The guanidine group of Arg152 have binding affinities to the hydrophilic nature of the inhibitors (−OH and = O groups). 1−(2,4−dihydroxyphenyl)−3,3−diphenylpropan−1−one was found to be most fitted ligand in active cavity of ADH29478 which includes active site residue. This information might be useful in designing new neuraminidase inhibitor for rapidly mutating H1N1 strains with high potency.
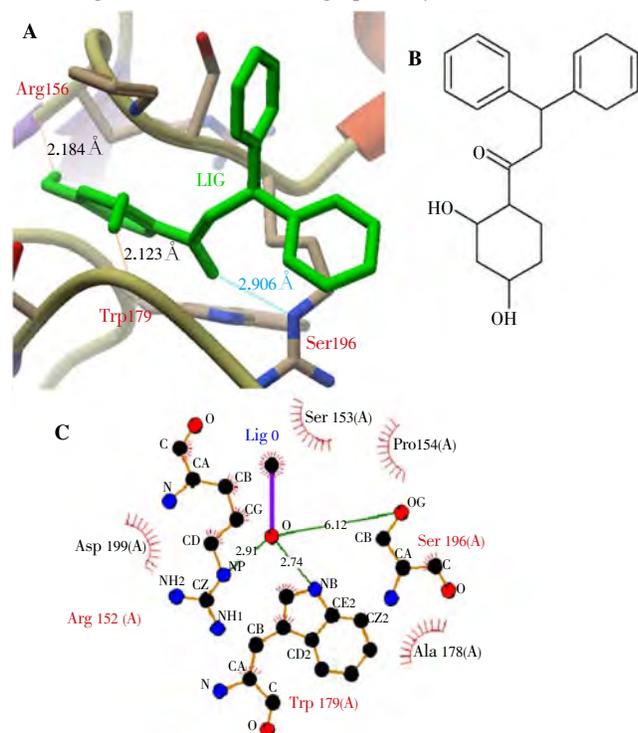
binding pocket cavity of AFO38701 (Table 2, Figure 5). The total intermolecular energy was −10.75 kcal/mol and more interestingly the inhibition constant value of 0.445 μmol/L. This signifies that it may have good inhibition potential than other FDA approved drugs. 1−(2,4−dihydroxyphenyl)−3,3−diphenylpropan−1−one was again found interacting with 150 loop region in the vicinity of active site residues which is responsible for catalytic activity of neuraminidase.
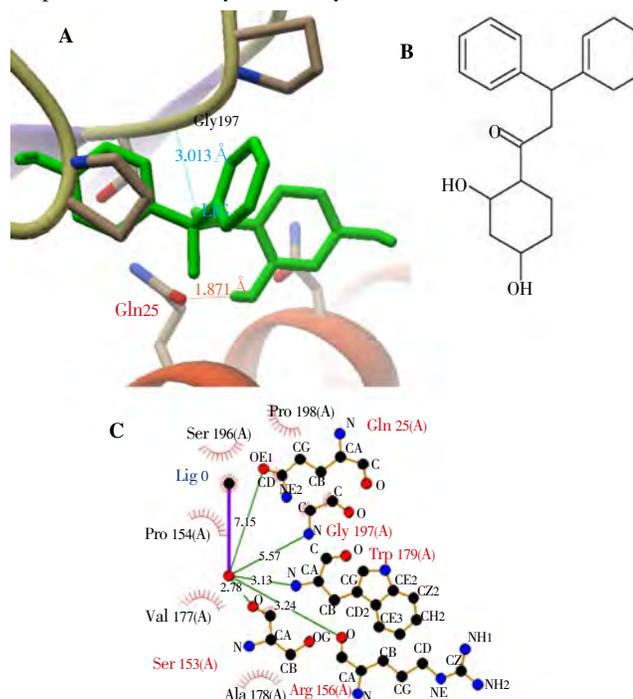

Figure 4. A−Docked ligand (CID: 19875815) with Chennai, B−Chemical structure of ligand, C−Ligplot interaction.

Figure 5. A−Docked ligand (CID: 19875815) with Gwalior, B−Chemical structure of ligand, C−Ligplot interaction.

3.2.2. Molecular interaction between 4−hydroxypanduratin A derivatives with neuraminidase of AFO38701 from Gwalior

The molecular interaction analysis between 4−hydroxypanduratin A derivatives with neuraminidase of AFO38701 from Gwalior was also done and on the basis of molecular interactions shown by ligplot and docking 1−(2,4−dihydroxyphenyl)−3,3−diphenylpropan−1−one (CID: 19875815) was again identified as best lead compound. It was found interacting with binding energy of −8.66 kcal/mol, 05 hydrogen bond interaction with Gln25, Gly197, Ser153, Trp179, Arg156 and 05 hydrophobic interactions in the active

3.2.3 Molecular interaction between 4−hydroxypanduratin A derivatives with neuraminidase of AEM62864 from Pune

Additionally, the molecular interactions analysis between 4−hydroxypanduratin A derivative 1−(2,4−dihydroxyphenyl)−2−phenylpropan−1−one with neuraminidase of AEM62864 from Pune identified by ligplot and docking revealed CID: 10776540 as second best lead compound. The binding energy was found to be −5.33 kcal/mol, 04 hydrogen bond interaction with Asp151, Lys150, Gln136, His144 and 03 hydrophobic interactions in the active binding pocket cavity of AEM62864 (Table 3, Figure 6). The total intermolecular energy was −6.83

Table 2

Characteristics of top 5 4−hydroxypanduratin A derivative inhibitors of neuraminidase H1N1 [AFO38701 (Gwalior)] identified after molecular docking.

CID	Molecular formulae	M. W (g/mol)	Log P	Binding Energy score (kcal/mol)	Total inhibition constant Ki (μmol/L) at 298.15 K	Hydrophobic bond interaction	Hydrogen bond interaction	Total intermolecular energy (kcal/mol)
19875815	$C_{21}H_{18}O_3$	318.36	4.8	−8.66	0.445	5 (Gln25, Gly197, Ser153, Trp179, Arg156)	5	−10.75
21680120	$C_{17}H_{18}O_4$	286.32	3.8	−8.57	0.525	7 (Gln25, Gly197, Ser153, Trp179, Ser196, Val177)	5	−10.06
42607676	$C_{20}H_{22}O_4$	326.38	4.9	−8.28	856.01	2 (Trp179, Gln25)	8	−10.16
66691619	$C_{16}H_{16}O_4$	272.29	3.6	−7.50	3.17	3 (Trp179, Gln25, Ser196)	6	−9.59
57524956	$C_{25}H_{28}O_5$	408.48	4.6	−7.46	3.40	3 (Asp199, Arg152)	8	−10.14
65028	$C_{16}H_{28}N_2O_4$	312.40	1.1	−6.30	23.97	1 (Trp179)	8	−8.99
154234	$C_{15}H_{28}N_4O_4$	328.40	0	−5.05	199.11	4 (Asp199, Arg152, Asp151)	3	−7.73
60855	$C_{12}H_{20}N_4O_7$	332.30	−3.2	−6.01	39.65	2 (Trp179, Arg152)	4	−8.99

Osel=Oseltamivir, Per=Peramivir, Zan=Zanamivir.

Table 3

Characteristics of top 5 4–hydroxypanduratin A derivative inhibitors of neuraminidase H1N1 [AEM62864 (Pune)] identified after molecular docking.

CID	Molecular formulae	M. W. (g/mol)	Log P	Binding Energy score (kcal/mol)	Total inhibition constant Ki(μmol/ L) at 298.15 K	Hydrogen bond interaction	Hydrophobic bond interaction	Total intermolecular energy (kcal/mol)
10776540	$C_{15}H_{14}O_3$	242.26	3.6	−5.33	123.14	4 (Asp151, Lys150, Gln136, His144)	3	−6.83
19744862	$C_{20}H_{24}O_5$	344.40	4.8	−5.21	152.91	2 (Asn146, Lys150)	5	−8.49
21600667	$C_{14}H_{12}O_5$	261.23	2.3	−5.21	151.50	4 (Ser176, Phe196, Lys207)	3	−7.30
21598932	$C_{26}H_{24}O_7$	448.46	4.3	−4.54	471.26	1 (Lys207)	8	−7.52
20225615	$C_{22}H_{26}O_6$	386.43	5.4	−4.10	988.14	1 (Lys262)	5	−8.57
65028	$C_{16}H_{28}N_2O_4$	312.40	1.1	−5.14	169.71	2 (Ser153, Lys150)	7	−7.83
154234	$C_{15}H_{28}N_4O_4$	328.40	0	−3.43	3050	2 (Ser176, Lys207)	5	−6.12
60855	$C_{12}H_{20}N_4O_7$	332.30	−3.2	−3.22	4330	5 (Ser176, Val205, Val177, Phe 176, Lys207)	0	−6.21

Osel= Oseltamivir, Per= Peramivir, Zan= Zanamivir.

kcal/mol and more interestingly the inhibition constant value of 123.14 μmol/L. This signifies that it would have also good inhibition potential than other selected drugs.
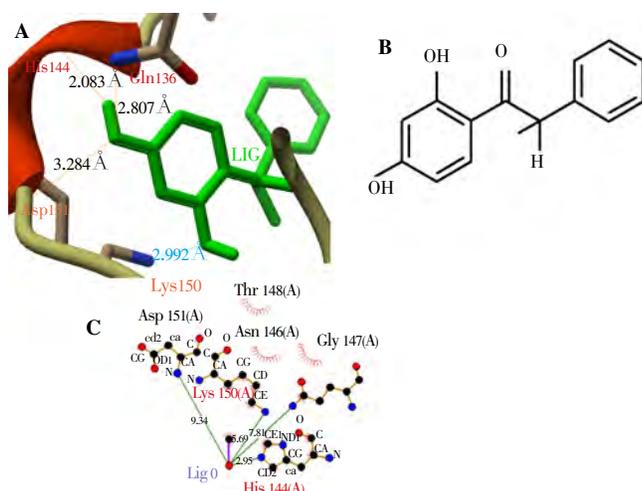

Figure 6. A–Docked ligand (CID: 10776540) with Pune, B–Chemical structure of ligand, C–Ligplot interaction.

4. Discussion

Influenza A viral infection is still a major health concern, and the options for the control and treatment of the disease are limited. The threat of a new pandemic requires the development of new therapeutic agents. Antiviral drugs are prescribed medicines against viral infections, including swine flu and influenza virus. In the present stud,y the conserved neuraminidase residues have been targeted to block associated neuraminidase activity. On the basis of molecular interactions of herbal compound 1–(2,4–dihydroxyphenyl)–3,3–diphenylpropan–1–one was identified as the best lead compound. The binding energy was found to be −7.40 kcal/mol, which is higher than FDA approved drugs *viz.*, oseltamivir, zanamivir and peramivir. A higher value of negative interaction energy is an indicator of more efficient interaction between the protein and the neuraminidase inhibitors. 03 hydrogen bond interaction with residues Arg152, Trp179 and Ser196 were found in the binding pocket

of ADH29478 and most interestingly the inhibition constant value of 3.75 μmol/L much lower (*i.e.* 45 times) than other selected FDA approved bio–drugs for swine flu signifies high inhibition potential of 1–(2,4–dihydroxyphenyl)–3,3–diphenylpropan–1–one. Additionally, this herbal compound was found interacting with 150 loop region, which are responsible for catalytic activity of neuraminidase, very near to binding cavity, such that it recognizes to enable more extensive interactions with the ligand, as well as with other active–site residues in the vicinity. The top hits have shown high binding affinity than the FDA approved drugs such as oseltamivir, zanamivir, and peramivir. Therefore, this analysis revealed the importance of computational approaches drug designing and discovery. This study proposes to put forward a constructive conception to designing a neuraminidase H1N1 inhibitors such as 1–(2,4–dihydroxyphenyl)–3,3–diphenylpropan–1–one.

Conflict of interest statement

We declare that we have no conflict of interest.

Acknowledgements

Comments

Background

This is an important paper in the field of Indian H1N1

influenza neuraminidase. The study is directed to find the neuraminidase H1N1 (swine flu) inhibition potential of 4–hydroxypanduratin A and its derivatives along with associated binding mechanism through virtual screening and molecular docking.

Research frontiers

Studies are being performed in order to determine which may be the significant herbal inhibitors of neuraminidase H1N1 reported in India in 2000–2013. Modeller 10.11 and I–TASSER server have been used for 3D structure prediction and virtual screening along with molecular docking studies have been performed to find out ligand and protein interaction and have been compared with other FDA approved drugs such as oseltamivir, zanamivir, and peramivir for inhibitory potential.

Related reports

The data about neuraminidase H1N1 have been collected from NCBI Influenza virus resources. The results are agreement and good as compared to other FDA approved drugs such as oseltamivir, zanamivir, and peramivir for inhibitory potential is probably due to the similar binding mechanism and with same active site residues. 4–hydroxypanduratin A has shown promising inhibitory activity against dengue virus NS2B/NS3 protease (Kiat *et al.*, 2006 and Frimayanti *et al.*, 2011) and Japanese encephalitis virus, a major cause of acute encephaltis in Asia (Seniya *et al.*, 2013), hence it may be a potential inhibitor of neuraminidase H1N1.

Innovations & breakthroughs

The guanidine group of residues Arg152 and Trp179 of ADH29478 (Chennai) and AFO38701 (Gwalior) neuraminidase models hydrophilic domain (−OH and =O groups) were identified to have molecular interactions with high binding affinity energy of −7.40 kcal/mol and −8.66 kcal/mol, respectively to 1–(2,4–dihydroxyphenyl)–3,3–diphenylpropan–1–one (CID: 19875815) than other FDA approved drugs such as oseltamivir, zanamivir, and peramivir. This study has shown that 1–(2,4–dihydroxyphenyl)–3,3–diphenylpropan–1–one will be a breakthrough for further drug development against swine flu.

Applications

It may be significant to know the distribution of resistance to other FDA approved drugs against neuraminidase H1N1 virus from India as well as in the world. Hence, due to resistance of H1N1 virus, it is quite good to identify new therapeutic compounds and especially from natural sources. The results of the present study suggest that herbal compound 1–(2,4–dihydroxyphenyl)–3,3–diphenylpropan–1–one may act as a significant inhibitor of neuraminidase H1N1 as compared to other FDA approved drugs with high potency. Thus, it is important to estimate further drug development of therapeutic compounds against neuraminidase H1N1 virus.

Peer review

This is a good study in which the authors evaluated the molecular interactions of herbal compound into active site residues of neuraminidase H1N1 which are responsible for catalytic activity. The results are interesting and suggested that 1–(2,4–dihydroxyphenyl)–3,3–diphenylpropan–1–one may act as a significant inhibitor of neuraminidase H1N1 as compared to other FDA approved drugs.

References

[1] Yun JM, Kwon H, Hwang JK. *In vitro* anti–inflammatory activity of pandurain A isolated from *Kaempferia pandurata* in RAW264.7 cells. *Planta Med* 2003; **69**(12): 1102–1108.

[2] Lai SL, Cheah SC, Wong PF, Noor SM, Mustafa MR. *In vitro* and in vivo anti–angiogenic activities of Panduratin A. *PLoS One* 2012; **7**(5): e38103.

[3] Fahey JW, Stephenson KK. Pinostrobin from honey and Thai ginger (*Boesenbergia pandurata*): a potent flavonoid inducer of mammalian phase 2 chemoprotective and antioxidant enzymes. *J Agric Food Chem* 2002; **50**(25): 7472–7476.

[4] Shindo K, Kato M, Kinoshita A, Kobayashi A, Koike Y. Analysis of antioxidant activities contained in the *Boesenbergia pandurata* Schult. Rhizome. *Biosci Biotechnol Biochem* 2006; **70**(9): 2281–2284.

[5] Kiat TS, Pippen R, Yusof R, Ibrahim H, Khalid N, Rahman NA. Inhibitory activity of cyclohexenyl chalcone derivatives and flavonoids of fingerroot, *Boesenbergia rotunda* (L.), towards dengue–2 virus NS3 protease. *Bioorg Med Chem Lett* 2006; **16**(12): 3337–3340.

[6] Frimayanti N, Chee CF, Zain SM, Rahman NA. Design of new competitive dengue ns2b/ns3 protease inhibitors–a computational approach. *Int J Mol Sci* 2011; **12**(2): 1089–1100.

[7] Seniya C, Mishra H, Yadav A, Sagar N, Chaturvedi B, Uchadia K, et al. Antiviral potential of 4–hydroxypanduratin A, secondary metabolite of Fingerroot, *Boesenbergia pandurata* (Schult.), towards Japanese encephalitis virus NS2B/NS3 protease. *Bioinformation* 2013; **9**(1): 54–60.

[8] Wang SQ, Du QS, Huang RB, Zhang DW, Chou KC. Insights from investigating the interaction of oseltamivir (Tamiflu) with neuraminidase of the 2009 H1N1 swine flu virus. *Biochem Biophys Res Commun* 2009; **386**: 432–436.

[9] Nguyen HT, Fry AM, Gubareva LV. Neuraminidase inhibitor resistance in influenza viruses and laboratory testing methods. *Antivir Ther* 2012; doi: 10.3851/IMP2067.

[10] Wang SQ, Du QS, Chou KC. Study of drug resistance of chicken influenza A virus (H5N1) from homology–modeled 3D structures of neuraminidase. *Biochem Biophys Res Commun* 2007; **354**(3): 634–640.

[11] Wang YT, Chan CH, Su ZY, Chen CL. Homology modeling, docking, and molecular dynamics reveal HR1039 as a potent inhibitor of 2009 A (H1N1) influenza neuraminidase. *Biophys Chem* 2010; **147**(1–2): 74–80.

[12] Liu H, Yao X, Wang C, Han J. *In silico* identification of the potential drug resistance sites over 2009 influenza A (H1N1) virus neuraminidase. *Mol Pharm* 2010; **7**(3): 894–904.

[13] Amaro RE, Swift RV, Votapka L, Li WW, Walker RC, Bush RM. Mechanism of 150–cavity formation in influenza neuraminidase. *Nat Commun* 2011; doi: 10.1038/ncomms1390.

[14] Pan D, Sun H, Bai C, Shen Y, Jin N, Liu H, et al. Prediction of zanamivir efficiency over the possible 2009 influenza A (H1N1) mutants by multiple molecular dynamics simulations and free energy calculations. *J Mol Model* 2011; **17**(10): 2465–2473.

[15] Chavan S, Bhayye S, Sobhia ME. Molecular dynamics directed CoMFA studies on carbocyclic neuraminidase inhibitors. *Mol Divers* 2011; **15**(4): 979–987.

[16] Mai BK, Li MS. Neuraminidase inhibitor R–125489––a promising drug for treating influenza virus: steered molecular dynamics approach. *Biochem Biophys Res Commun* 2011; **410**(3): 688–691.

[17] Collins PJ, Haire LF, Lin YP, Liu J, Russell RJ, Walker PA, et al. Crystal structures of oseltamivir–resistant influenza virus neuraminidase mutants. *Nature* 2008; **453**(7199): 1258–1261.

[18] Hauge SH, Dudman S, Borgen K, Lackenby A, Hungnes O. Oseltamivir–resistant influenza viruses A (H1N1), Norway, 2007–08. *Emerg Infect Dis* 2009; **15**(2): 155–162.

[19] Moscona A. Global transmission of oseltamivir–resistant influenza. *N Engl J Med* 2009; **360**(10): 953–956.

[20] van der Vries E, Veldhuis Kroeze EJ, Stittelaar KJ, Linster M, Van der Linden A, Schrauwen EJ, et al. Multidrug resistant 2009 A/H1N1 influenza clinical isolate with a neuraminidase I223R mutation retains its virulence and transmissibility in ferrets. *PLoS Pathog* 2011; **7**(9): e1002276.

[21] Kokh DB, Wade RC, Wenzel W. Receptor flexibility in small–molecule docking calculations. *Wiley Interdiscip Rev: Comput Mol Sci* 2011; **1**(2): 298–314.

[22] Bao Y, Bolotov P, Dernovoy D, Kiryutin B, Zaslavsky L, Tatusova T, et al. The influenza virus resource at the National Center for Biotechnology Information. *J Virol* 2008; **82**(2): 596–601.

[23] Sali A, Blundell TL. Comparative protein modelling by satisfaction of spatial restraints. *J Mol Biol* 1993; **234**(3): 779–815.

[24] Laskowski RA, MacArthur MW, Moss DS, Thornton JM. PROCHECK: a program to check the stereochemical quality of protein structures. *J Appl Cryst* 1993; **26**: 83–91.

[25] Dundas J, Ouyang Z, Tseng J, Binkowski A, Turpaz Y, Liang J. CASTp: computed atlas of surface topography of proteins with structural and topographical mapping of functionally annotated residues. *Nucleic Acids Res* 2006; **34**: W116–W118.

[26] Liang J, Edelsbrunner H, Woodward C. Anatomy of protein pockets and cavities: measurement of binding site geometry and implications for ligand design. *Protein Sci* 1998; **7**(9): 1884–1897.

[27] Laurie AT, Jackson RM. Q–SiteFinder: an energy–based method for the prediction of protein–ligand binding sites. *Bioinformatics* 2005; **21**(9): 1908–1916.

[28] Lipinski CA, Lombardo F, Dominy BW, Feeney PJ. Experimental and computational approaches to estimate solubility and permeability in drug discovery and development settings. *Adv Drug Deliv Rev* 2001; **46**(1–3): 3–26.

[29] Morris GM, Huey R, Lindstrom W, Sanner MF, Belew RK, Goodsell DS, et al. AutoDock4 and AutoDockTools4: Automated docking with selective receptor flexibility. *J Comput Chem* 2009; **30**(16): 2785–2791.

[30] Seniya C, Yadav A, Uchadia K, Kumar S, Sagar N, Shrivastava P, et al. Molecular docking of (5E)–3–(2–aminoethyl)–5–(2–thienylmethylene)–1, 3–thiazolidine–2, 4–dione on HIV–1 reverse transcriptase: novel drug acting on enzyme. *Bioinformation* 2012; **8**(14): 678–683.

[31] Zhang Y. I–TASSER server for protein 3D structure prediction. *BMC Bioinformatics* 2008; doi:10.1186/1471–2105–9–40.

[32] Jones DT. Protein secondary structure prediction based on position–specific scoring matrices. *J Mol Biol* 1999; **292**(2): 195–202.

[33] Wu S, Zhang Y. LOMETS: a local meta–threading–server for protein structure prediction. *Nucleic Acids Res* 2007; **35**(10): 3375–3382.

[34] Wu S, Skolnick J, Zhang Y. *Ab initio* modeling of small proteins by iterative TASSER simulations. *BMC Biol* 2007; **5**: 17.

[35] Zhang Y, Kolinski A, Skolnick J. TOUCHSTONE II: a new approach to ab initio protein structure prediction. *Biophys J* 2003; **85**(2): 1145–1164.

[36] Xu D, Zhang Y. *Ab initio* protein structure assembly using continuous structure fragments and optimized knowledge–based force field. *Proteins* 2012; **80**(7): 1715–1735.

[37] Zhang Y, Skolnick J. SPICKER: a clustering approach to identify near–native protein folds. *J Comput Chem* 2004; **25**(6): 865–871.

[38] Zhang Y, Skolnick J. TM–align: a protein structure alignment algorithm based on the TM–score. *Nucleic Acids Res* 2005; **33**(7): 2302–2309.

[39] Zhang Y, Skolnick J. Automated structure prediction of weakly homologous proteins on a genomic scale. *Proc Natl Acad Sci USA* 2004; **101**(20): 7594–7599.

[40] Zhang Y, Skolnick J. Scoring function for automated assessment of protein structure template quality. *Proteins* 2004; **57**(4): 702–710.

[41] Meng XY, Zhang HX, Mezei M, Cui M. Molecular docking: a powerful approach for structure–based drug discovery. *Curr Comput Aided Drug Des* 2011; **7**(2): 146–157.